Martin Pietsch, Anja Klein and Florian Steinke, ”Merging Microgrids for Optimal Distribution Grid Restoration under Explicit Communication Constraints,” in *Proc. of the IEEE Resilience Week (RWS) 2020 Symposium*, November 2020.

Merging Microgrids for Optimal Distribution Grid Restoration under Explicit Communication Constraints

1st Martin Pietsch
Technische Universität Darmstadt
Darmstadt, Germany
martin.pietsch@eins.tu-darmstadt.de

2nd Anja Klein
Technische Universität Darmstadt
Darmstadt, Germany
a.klein@nt.tu-darmstadt.de

3rd Florian Steinke
Technische Universität Darmstadt
Darmstadt, Germany
florian.steinke@eins.tu-darmstadt.de

***Abstract*—Distributed generators offer the possibility for fast power grid restoration after disastrous events by forming local microgrids. Merging such microgrids increases the supply capacity for critical loads which cannot be supplied by one generator individually. This step, however, requires an active communication channel between the involved distributed generators for continued stable operation. We show in this paper how to compute optimal restoration sequences, that explicitly take into account this interdependency between the electrical and the communication network when merging local microgrids. We demonstrate our approach on a basic example and an adapted version of the IEEE 123-node test feeder, showing that our approach allows resupplying significantly more and larger loads compared to isolated microgrid operation.**

***Index Terms*—distribution grid restoration, communication constraints, multilayer grid, mixed-integer-linear-programming**

I. Introduction

Smart distribution grids with decentral generation and active consumers are an adequate way to integrate renewable energies into power systems [1]. Their dependence on digitalised infrastructure, however, implies an increasing risk for cyber attacks [2], [3] and supply resilience is thus an important, timely topic. This claim is underlined by the growing number of extreme weather events [4]. One answer to this challenge is the use of smart grids' distributed generators (DGs) to form local microgrids. This offers significant potential to endure and overcome the disastrous consequences of long-term power outages. For example, local microgrids were used to ensure emergency supplies in the aftermath of the earthquake and the following tsunami in Japan in 2011 [5], [6].

The optimal segmentation of a power distribution grid into separate microgrids – one for each DG – can be computed by solving a mixed integer linear program (MILP), where it is assumed that all line segments are switchable [7]. The approach can be extended to switching sequences and unbalanced power networks employing approximate AC power flow models [8], to include power support by decentral renewable sources and the effects of cold load pickup [9], and to the scheduling of mobile generators and repair crews [10]. All these works considered only one generator per microgrid, or at least only in one location over the whole time set [10]. Merging multiple microgrids into one by connecting their distributed generators, however, has significant advantages. It allows to supply larger loads which could not be supplied by one generator alone, increases the amount of available reserve power during the restoration process and offers at least some redundancy towards additional outages of one of the DGs.

The key assumption of this paper is that the continued stable operation of multiple cooperative DGs in one microgrid requires a communication channel between these generators. Primary load balancing is typically performed via frequency control, implemented by decentral proportional controllers without communication [11]. While this scheme works for short periods of time, a secondary frequency control scheme is required to restore the system frequency back to nominal values and free the primary reserves to handle further power imbalances. The secondary control scheme, typically implemented as a proportional integrating (PI) controller, can be run on one DG only, but this implies that only this generator's capacity is available for secondary reserve. Running non-communicating PI-controllers on multiple DGs in parallel is instable. Therefore, one typically uses only one centralized PI controller [11] or decentralized consensus-based version thereof [12], [13]. Both of these approaches, however, require a communication channel between the generators.

In this paper we distinguish between "slow" and "fast" communication channels. Several slow communication channels offer limited information exchange capabilities, i.e. low data rates and high latencies, even under the restricted conditions of a blackout. Long Range Wide Area Networks (LoRaWAN) are designed for low energy consumption and can survive on battery support for long periods of time. Other options include direct communication via personal transport (e.g. by car) or peer-to-peer solutions using mobile end devices [14]. These slow communication paths are not suitable for the control of cooperatively operating DGs. They do, however, offer possibilities for obtaining situational awareness, for commanding a limited number of switching operations, or for distributing restoration plans. To enable stable DG cooperation, higher data rates and lower latencies of a "fast" communication channel

978-1-7281-8693-1/20/$31.00 ©2020 IEEE

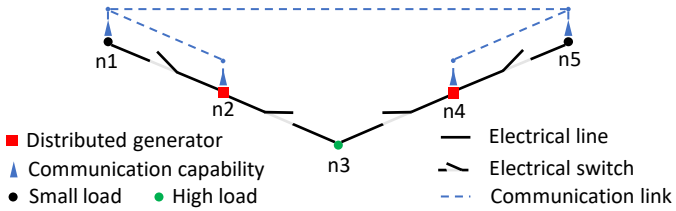

Fig. 1. Topology of a 5-node test grid, showing the connected electrical and communication grid. In order to sequentially restore all loads of the grid both DG have to synchronize their generation to ensure safe merging of the two initialized microgrids.

are needed. Such communication can be provided by wired or mobile infrastructure-based networks. While mobile base stations are typically equipped with backup energy supplies to bridge short blackouts periods, they cannot stay operational during longer outages. In some areas specific radio frequency bands are reserved for public protection and disaster relief [15] and special networks of corresponding radio antennas with extended energy supplies are installed. However, such networks are not available everywhere and should save their capacity for other emergency services. Satellite telephony may be another option, but is rarely available in distribution grids. In summary, we find that the most fast communication channels require dedicated power support for extended operation during a blackout.

Several scientific works on distribution grid restoration assume communication capabilities without taking into account the interdependence of communication and its power supply [10], [16]–[18]. [7] investigates the use of slow communication between local agents to obtain status data about the network situation after a disastrous event. Cooperative operation of multiple DGs subject to a communication link to grid-external central communication points is discussed in [19]. The ability to compensate power shortages between different microgrids, which are connected via a central communication point, is investigated in [20]. All these approaches show the importance of communication, but do not address the dependence of communication itself on power supply.

In this paper, we formulate an algorithm for the sequential restoration of distribution networks, considering an explicit model of the communication grid topology between the generators and the electrical supply thereof during the restoration phase. Generators in distinct microgrids are allowed to cooperate – effectively merging the microgrids – only after a fast communication link between them has been established. For a demonstrative example see Fig. 1. The contribution of this paper is to show how this condition can be included into a MILP-based restoration planning approach. Compared to previous work, that requires tracking the electrical and communication affiliation status between all nodes and the generators throughout the restoration process. Moreover, we need to formulate specific novel constraints based on these values. The reward for this effort is to make the harvesting of the aforementioned benefits of cooperative DG control more realistic.

In Section II, we describe the key modeling steps of the paper, before presenting the restoration optimization problem in Section III. In Section IV, we present the exemplary optimization results both for the demonstrative example in Fig. 1 and an adapted version of the IEEE 123-node test feeder. Section V concludes with a summary and an outlook.

II. Key Modeling Steps

Before describing the optimization problem for the restoration sequence in detail in Section III, we present key modeling concepts with respect to the electrical and the communication infrastructure, the restoration process, and our computational setup in this section.

A. Electrical Infrastructure & Restoration Process

Let the electrical distribution network consist of nodes $i, j \in \mathcal{N} = \{1, 2, ..., N\}$ and electrical lines $(i, j) \in \mathcal{L}^E = \{(i, j) : i, j \in \mathcal{N}\}$. Each node i can be in an energized state at time $t \in \mathcal{T} := \{1, 2, ..., T\}$, denoted as $\alpha^E_{i,t} = 1$, or blacked out, denoted as $\alpha^E_{i,t} = 0$. Node i has a power demand of d_i, and we assume in line with [7] that progressing automation of power grids will lead to the switchability of all loads and lines. We denote a closed load switch at node i and time t by $u^E_{i,t} = 1$. We also assume that all lines are switchable and let $u^E_{ij,t} = 1$ indicate a connected line between nodes i and j at time t.

Initially all loads and lines are assumed to be disconnected after a blackout. The grid is then restored starting from a set of black-start/grid-forming capable DGs $\mathcal{G} \subseteq \mathcal{N}$. By sequentially re-closing line switches, more and more nodes are energized thereafter. Whenever a node is energized and the supplying generators have sufficient free active power available, its local load switch can be closed such that the local load demand is resupplied.

In the experiments of this work we consider all lines and switches to be operational at all times. In effect, we examine a local resupply scenario after an outage in the upper voltage levels. Damaged, destroyed, or blocked components within the modeling domain could additionally be incorporated by forcing some switching variables to fixed values [7], [8]. Unlike various previous works [7], [21], [22], we do not restrict the network to be radial.

B. Communication Infrastructure

We assume that some nodes of the electric grid also have communication capabilities, allowing them to establish fast communication links to other nodes. This defines the communication graph with the same node set $\mathcal{N}$ as the electric graph and the possible communication links $(i, j) \in \mathcal{L}^C$ as edges. $\mathcal{L}^C$ and $\mathcal{L}^E$ need not to express the same topology. In fact, they will often be different in practice.

Whenever both end nodes of a communication link were energized at the time $t - 1$, the link is assumed to become operational at time t, indicated by $\alpha^C_{ij,t} = 1$ for the link between nodes i and j. An active communication link at one node i does not presuppose a closed load switch for the load demand at that node, i.e. $u^E_{i,t} = 1$. Instead, the DGs

that energize node i are assumed to always have sufficient power reserves to additionally support the energy demand for the communication capability without this being explicitly modeled. This is plausible since communications' energy demand is typically small compared to the other loads in the system.

C. Computational Considerations

Our optimization formulation for computing restoration sequences takes a central perspective: it calculates the optimal switching sequence for the entire network given the pre-fault load values at all network nodes (and potentially the damage status of all switches, lines and other equipment). This input information could be gathered via a "slow" communication system, as mentioned above. The computed switching sequences would have to be distributed in the same way. Alternatively, one could perform both steps in a distributed fashion using consensus protocols as explained in [7].

Our core assumption is that the cooperative operation of several DGs requires fast communication between them to operate synchronized and controlled. To prevent electrical lines, that would connect two microgrids whose generators do not have such a channel yet, from being activated we introduce the following formalism: we define binary variables $\chi^E_{ig,t}$ and $\chi^C_{ig,t}$ that denote for each node i at each time t whether or not it is connected to generator $g \in \mathcal{G}$ via active lines/links in the electrical (E) or the communication (C) network. To express this "affiliation" status via a set of mixed integer linear equations, we employ the method of fictitious single-commodity flows [23], which is described in detail in Section III-E.

We formulate the optimization as a MILP problem. This class of optimization problems is well-suited to model our switching conditions and can be optimized with powerful standard solvers. They often find feasible solutions very quickly and provide hard optimality guarantees throughout the optimization process.

Several previous studies considered detailed three-phase (unbalanced) AC power flow calculations for distribution network restorations with microgrids [8]–[10], [24]. To simplify our outline and to focus on our new additions, we restrict ourselves to a simple standard DC power flow model [25]. The model could, however, straight-forwardly be extended in line with the referenced work to include these additional aspects.

III. Optimization Formulation

We are now ready to formulate the MILP problem for computing an optimal sequence of switching operations to restore the grid after a blackout. To keep our notation compact, we define that an index without a set in a for-all statement means that the index runs over all possible values for that symbol, e.g., we write $\forall i$ instead of $\forall i \in \mathcal{N}$. If the index does not run over all possible values, we denote a corresponding condition or a value set explicitly.

A. Objective Function

The objective function is the weighted average restored load over the planning horizon,

$$max \, \frac{1}{T} \sum_{t \in T} \sum_{i \in N} w_i \cdot d_i \cdot u^E_{i,t}. \tag{1a}$$

This objective is equivalent to minimizing the average non-supplied load.

B. Electrical Constraints

The first condition for the electrical system is the energy balance at each node

$$\sum_{g \in \mathcal{G}} p_{g,t} \delta_{i,g} - d_i \cdot u^E_{i,t} = \sum_{j \in \Omega^E_i} p_{ij,t} \ , \forall i, t. \tag{2a}$$

Here, $p_{g,t}$ is the power output of DG g at time t, $p_{ij,t}$ the power flow from node i to node j at time t, and Ω^E_i the set of neighbours of node i in the electrical graph .

Generators have capacity limits $\overline{p}_g$, implying

$$0 \leq p_{g,t} \leq \overline{p}_g \ , \forall g, t. \tag{2b}$$

Similarly, we use the big-M method to restrict line power flows depending on their switching status $u^E_{ij,t}$ as

$$-\overline{p}_{ij} \cdot u^E_{ij,t} \leq p_{ij,t} \leq \overline{p}_{ij} \cdot u^E_{ij,t} \ , \forall t, i, j \in \Omega^E_i, \tag{2c}$$

where $\overline{p}_{ij}$ denotes the maximum power capacity of the line between node i and j.

Employing DC power flow modeling, we assume that

$$p_{ij,t} = B_{ij} \left(\theta_{i,t} - \theta_{j,t} \right) - s_{ij,t} \ , \forall t, i, j \in \Omega^E_i \ , \tag{2d}$$

where B_{ij} is the admittance matrix value between nodes i and j and $\theta_{i,t}$ the voltage phase angle at nodes i and time t. The slack variable $s_{ij,t}$ allows to have independent phase angles at the ends of disconnected lines. Using a big-M construction again we require

$$-M \cdot (1 - u^E_{ij,t}) \leq s_{ij,t} \leq M \cdot (1 - u^E_{ij,t}), \quad \forall t, i, j \in \Omega^E_i, \tag{2e}$$

for sufficiently large M. We set M to the cardinality of $\mathcal{N}$ in our experiments. Though not strictly needed, we found the following additional anti-symmetry constraint to significantly speed up computations,

$$p_{ji,t} = -p_{ij,t} \ , \forall t, i, j \in \Omega^E_i. \tag{2f}$$

C. Energization & Link Activation Status

A node can be energized if it is electrically affiliated with at least one generator,

$$\alpha^E_{i,t} \leq \sum_{g \in \mathcal{G}} \chi^E_{ig,t} \ , \forall i, t \ . \tag{3}$$

A communication link can only be active if both end points were energized in the timestep before,

$$2 \cdot \alpha^C_{ij,t} \leq \alpha^E_{i,t-1} + \alpha^E_{j,t-1} \ , \forall t > 1, i, j \in \Omega^C_i. \tag{4}$$

Once a node is energized it stays energized for the rest of the time,

$$\alpha^E_{i,t} \geq \alpha^E_{i,t-1}, \forall i, t > 1. \tag{5}$$

D. Switching Constraints

Reconnecting local loads is limited by the energization status,

$$u^E_{i,t} \leq \alpha^E_{i,t} \ , \forall i, t. \tag{6}$$

Concerning line switching decisions, we state that an electrical line can only be activated if at least one of the two end points was energized in the time step before,

$$u^E_{ij,t} \leq \alpha^E_{i,t-1} + \alpha^E_{j,t-1} \ , \forall t > 1, i, j \in \Omega^E_i. \tag{7a}$$

This allows to electrically connect to non-energized nodes. When an electrical line is activated, both end points are energized,

$$\begin{aligned} \alpha^E_{i,t} \geq u^E_{ij,t}, \forall t, i, j \in \Omega^E_i, \\ \alpha^E_{j,t} \geq u^E_{ij,t}, \forall t, i, j \in \Omega^E_i. \end{aligned} \tag{7b}$$

Once a line switch is closed, it is not opened again,

$$u^E_{ij,t} \geq u^E_{ij,t-1} \ , \forall t > 1, i, j \in \Omega^E_i, \tag{7c}$$

and we assume symmetry,

$$u^E_{ij,t} = u^E_{ij,t} \ , \forall t, i, j \in \Omega^E_i. \tag{7d}$$

What remains is the core novel condition in this paper: two microgrids can only be merged if their generators are able to communicate. We express this as follows,

$$\begin{aligned} u^E_{ij,t} \leq (1 - \chi^E_{ig,t}) + (1 - \chi^E_{j\tilde{g},t}) \\ + \chi^C_{g\tilde{g},t-1} \ , \forall i, g, \tilde{g}, t > 1, j \in \Omega^E_i. \end{aligned} \tag{8}$$

If node i is electrically affiliated to generator g and node j to $\tilde{g} \in \mathcal{G}$, respectively, then g and $\tilde{g}$ must be affiliated in communication for the line switch between i and j to close.

The completeness of this condition is understood as follows: all of the inequalities (8) are trivially satisfied for $u^E_{ij,t} = 1$ if one of the endpoints is not electrically affiliated to any generator, i.e. $\chi^E_{ig,t} = 0$ for all $g \in \mathcal{G}$ or $\chi^E_{jg,t} = 0$ for all $g \in \mathcal{G}$. This, however, is not possible due to (7b) and (3) which jointly imply that there must be at least one electrical affiliation for both end nodes at time t. Another possibility for such unwanted behavior is that both end nodes are electrically affiliated to the same generator only, which would also trivially satisfy (8), since any generator is affiliated in communication with itself. However, this condition cannot hold for all segments on a path that electrically connects two distinct generators g and $\tilde{g}$. On at least one segment of the path, the end point nodes are electrically affiliated with g and $\tilde{g}$, respectively. This is due to fact that any generator is electrically affiliated with itself at all times. The conditions can therefore only hold in the whole network if any two DGs g and $\tilde{g}$ of a merged microgrid are affiliated in communication, which is exactly what we want to guarantee.

E. Affiliation Constraints

With the conditions in this section, we ensure that an electrical or communication affiliation between node i and generator g can only exist, if there is a connected/active path between i and g in the respective network. To this end, we use the fictitious commodity flow method [23]. For any generator g and both the electrical (E) and the communcation (C) grid we consider separate fictitious commodities. Such commodities flow from an infinite capacity source located at generator g over the connected/active network edges to fictitious demands of 1 for that commodity at all affiliated nodes i. Nodes that cannot be reached due to disconnected lines or inactive links thus cannot be affiliated.

This idea is formulated using the flow conservation conditions

$$\begin{aligned} -1 \cdot \chi^E_{ig,t} = \sum_{j \in \Omega^E_i} \Phi^E_{ij,g,t} \ , \forall g, t, i \neq g, \\ -1 \cdot \chi^C_{ig,t} = \sum_{j \in \Omega^C_i} \Phi^C_{ij,g,t} \ , \forall g, t, i \neq g, \end{aligned} \tag{9a}$$

where $\Phi^E_{ij,g,t}$ and $\Phi^C_{ij,g,t}$ are the flows of the respective commodity over line (i, j) at time t and Ω^E_i, Ω^C_i are the sets of electrical and communication neighbours of node i. The fact that only connected or active lines can be used for such flows is expressed as

$$\begin{aligned} -\mathcal{M} \cdot u^E_{ij,t} \leq \Phi^E_{ij,g,t} \leq \mathcal{M} \cdot u^E_{ij,t} \ , \forall i, g, t, j \in \Omega^E_i, \\ -\mathcal{M} \cdot \alpha^C_{ij,t} \leq \Phi^C_{ij,g,t} \leq \mathcal{M} \cdot \alpha^C_{ij,t} \ , \forall i, g, t, j \in \Omega^C_i. \end{aligned} \tag{9b}$$

We moreover assume anti-symmetry of the flows,

$$\begin{aligned} \Phi^E_{ij,g,t} = -\Phi^E_{ji,g,t}, \forall i, g, t, j \in \Omega^E_i, \\ \Phi^C_{ij,g,t} = -\Phi^C_{ji,g,t}, \forall i, g, t, j \in \Omega^C_i, \end{aligned} \tag{9c}$$

and once a node is affiliated, it stays affiliated for the rest of the time by:

$$\begin{aligned} \chi^E_{ig,t} \geq \chi^E_{ig,t-1}, \forall i, g, t > 1, \\ \chi^C_{ig,t} \geq \chi^C_{ig,t-1}, \forall i, g, t > 1. \end{aligned} \tag{9d}$$

For generators themselves we assume self-affiliation at all times, i.e.

$$\chi^E_{gg,t} = \chi^C_{gg,t} = 1, \forall g, t. \tag{9e}$$

F. Initialization Conditions

These conditions determine the state of the decision variables at time step $t = 1$ of the optimization problem. In a blackout situation we assume all switching variables to be zero initially, i.e. all switches of loads and lines are opened,

$$\begin{aligned} u^E_{ij,1} = 0, \forall i, j \in \Omega^E_i, \\ u^E_{i,1} = 0, \forall i. \end{aligned} \tag{10}$$

The combined problem is a MILP and can be solved efficiently with standard solvers. In order to avoid large generation jumps between consecutive timesteps, which might lead to dynamic instabilities in practice, one could include additional penalty terms or constraints to limit these. The same holds for avoiding large phase angle differences between adjacent

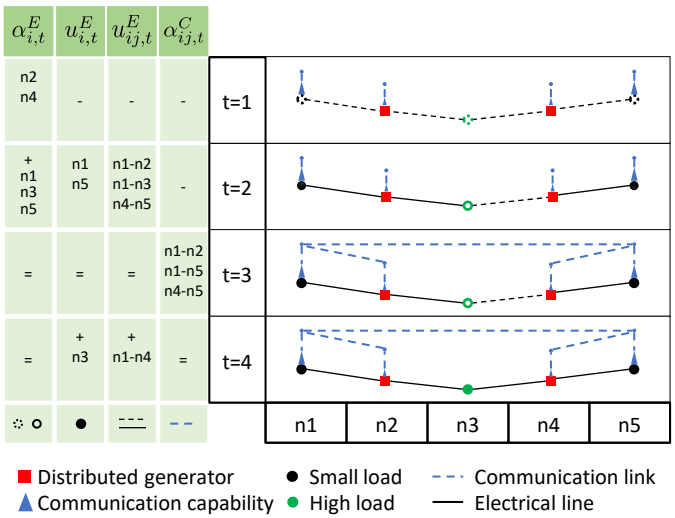

Fig. 2. Computed restoration sequence for the 5-node test grid shown in Fig. 1. A dashed node is not yet energized, a solid non-filled node is energized, a filled node additionally supplies its local load demand. Dashed electrical lines are disconnected whereas solid ones represent a closed line switch. Active communication links are shown a blue dashed, inactive ones are not shown. The high load can only be supplied after communication link between generators has been established.

nodes. Since our simulation environment does not react to these effects, we refrain from doing so in this paper.

IV. Simulation Results

In this section we present the results of the optimization problem for two systems. The first 5-node system, shown in Fig. 1, allows to illustrate the restoration sequence in detail. The second system is a modified version of the IEEE 123-node test feeder [26]. Thereafter, we shortly discuss computation times.

The MILP is optimized by the CPLEX solver with standard settings via the General Algebraic Modelling System (GAMS) [27]. The relative solution tolerance is set to 1%.

A. Case Study I: 5-Node Test Grid

The 5-node test grid consists of two DGs, two small loads and one high load. The small loads can be powered by a single DG alone, while the high load requires two DGs to work together to supply the load. The DGs have a rated power of $\overline{p}_{n2} = \overline{p}_{n4} = 250\,\text{kW}$. The small loads are $d_{n1} = d_{n5} = 100\,\text{kW}$, while the high load is d_{n3} $300\,\text{kW}$. The electrical line rating is $\overline{p}_{ij} = 250\,\text{kW}$ for all lines. All weights are set to $w_i = 1$ such that no node is preferred and the maximum load of the system shall be recovered. The topology of the communication network differs from the electrical network by the additional communication link between node $n1$ to $n5$ and the missing communication links to node $n3$.

The resulting switching sequence is shown in Fig. 2. After 4 timesteps the restoration process is complete. Initially all switchable elements are in an open state and the DG nodes are the only ones energized, starting two microgrids. In the second timestep the line switches $(n1, n2), (n2, n3), (n4, n5)$ are closed and the nodes connected to them $n1, n3, n5$ are energized. As there is no communication link between DG $n2$ and DG $n4$ yet, it is not possible to activate electrical line $(n3, n4)$, that would merge the two microgrids, at this time, see (8). The loads at nodes $n1$ and $n5$ are picked up ($u^E_{n1,2} = u^E_{n5,2} = 1$) and supplied by the respective DG. In the third timestep the communication links between the energized nodes are becoming active ($\alpha_{n1n5,3} = \alpha_{n1n2,3} = \alpha_{n2n3,3} = \alpha_{n4n5,3} = 1$). Due to the specific network structure, all possible links can be activated at once. In larger networks not all nodes would be energized in the first timestep already, and thus the communication network would sequentially be enlarged. In the fourth and last timestep synchronization of the DGs is possible as a result of the communication link established at time 3. Electrical line $(n3, n4)$ is thus activated ($u^E_{n3n4,4} = 1$) and load $n3$ can additionally be picked-up ($u^E_{n3,4} = 1$). Then, the network is completely restored. It is worth mentioning that in this particular case, due to the symmetric grid topology two optimal sequences can be obtained, by altering the closed lines $n2, n3$ and $n3, n4$ in $t2$ and $t3$.

B. Case Study II: Modified IEEE 123-Node Test Feeder Grid

We use the IEEE 123-node test feeder grid [26] as a basis and extend it with seven distributed DGs and a communication network as shown in Fig. 3. The topology of our model matches the IEEE test case and our nodal loads are represented as the sum of all phase loads of the IEEE grid. The highest loads are represented as green nodes in Fig. 3. They are also listed in Table I together with the power and location of the seven added DGs. In line with the IEEE data, the specific line reactance is assumed as $1.06\,\Omega/\text{mile}$. Using the original distances (the distance of nodes which were originally connected by switches were set to 100 ft) and a voltage level of $4.16\,\text{kV}$ we obtain the admittance matrix values B_{ij}. The power limits of the lines are set to the maximum power of the largest generator ($\overline{p}_{ij}$ = $1500\,\text{kW}$). Reducing the line limits will result in differently shared loads of the DGs, harder contraints and ultimately lead to infeasibility of the programm. The communication grid connects the nodes ($n6$, $n14$, $n20$, $n42$, $n66$, $n75$, $n88$, $n94$, $n106$) and seven DGs in a two-ring topology as shown in Fig. 3. We set the weights for all nodes to $w_i = 1$ and the time horizon to $T = 9$. The considered time horizon is defined in such a way that it is possible to restore all loads in the distribution network.

The restored load over the timesteps is shown in Fig. 4. In the first timestep, all DGs initialize local microgrids by energizing their nodes. Since all switches are open after a blackout situation, no loads are picked-up. After one timestep each microgrid is expanded by energizing the adjacent nodes, and the loads located at the DG node as well as the loads of the newly energized nodes are supplied. In the following timesteps, the picked up load and the number of energized nodes of each microgrid grows along the electrical topology until the microgrid reaches a node affiliated to another microgrid. When there is no communication path between the DGs

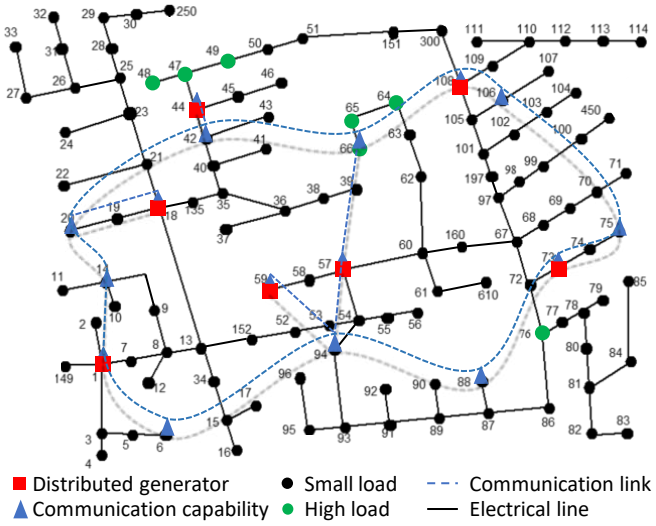

Fig. 3. Topology of the IEEE-123 node test feeder grid together with seven additional DGs and the assumed communication grid.

TABLE I
IEEE 123 NODE TEST FEEDER DG CAPACITY DATA AND HIGH LOADS

DG	Power [kW]	Nodes	Load [kW]
n1	250	n47	105
n18	500	n48	210
n44	300	n49	140
n57	220	n64	75
n59	1500	n65	140
n73	230	n66	75
n108	500	n76	245

of two such adjacent microgrids, no electrical connection can be established between them. This can be seen, for example, for microgrid DG-n59, which is limited in its expansion by DG-n57 until a communication link is formed. During that time, it only provides a power output of 40 kW. When node $n94$ is energized at $t = 3$, a communication connection between the DGs can be established at $t = 4$. The two DGs are then synchronized, whereupon both microgrids are merged from time $t = 5$ on and DG-n59 can provide higher power output. Since DG-n59 has much higher capacity (1500 kW) than DG-n57 (220 kW), the connection of both microgrids allows restoring many more network loads. An equivalent argumentation chain applies to DG-n18 and DG-n44. There again, the communication is formed in $t = 3$ and a connection between the microgrids is established at $t = 5$. This allows for the higher loads at the nodes $n47$, $n48$ and $n49$ to be supplied. At time $t = 9$ all loads of the distribution grid are restored.

For comparison, we consider the exact same network but without the communication links, thus without the option to merge microgrids. The results are shown in Fig. 5. Without cooperative operation of the DGs only 58 % of the total loads are recovered. One reason is that DG-n59 is limited to supply only 40 kW before its microgrid gets blocked by the microgrid

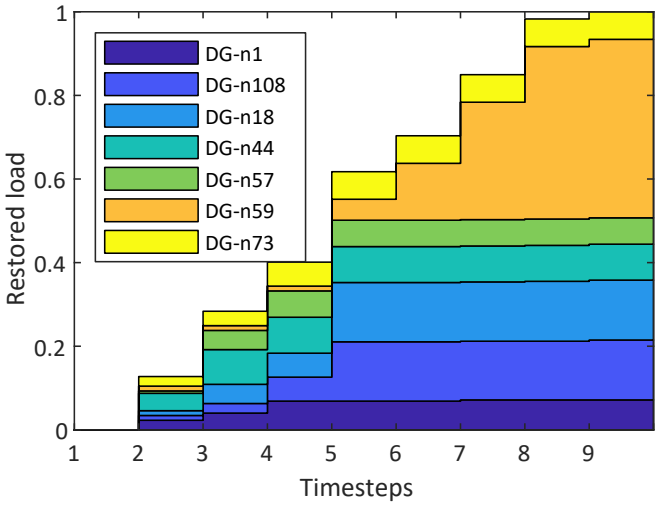

Fig. 4. Restored load and power output of each DG of the 123-node test-feeder over the time horizon of 9 timesteps, with microgrid merging. All load is restored after 9 timesteps. The benefit of the cooperative operation of DGs can be seen in timestep 5, where the restored load makes a significant jump.

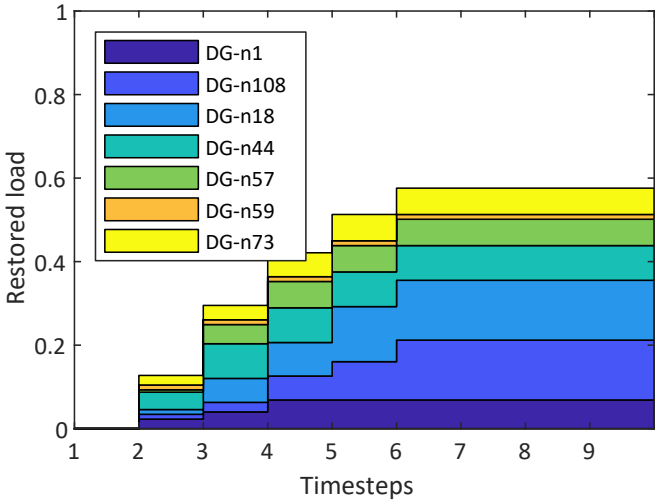

Fig. 5. Restored load and power output of each DG of the 123-node test-feeder over the time horizon of 9 timesteps, without microgrid merging. After 6 timesteps the maximum possible load (58%) is restored.

of DG-n57. Moreover, the higher loads at nodes $n48$ and $n76$ cannot be supplied.

The example shows that our approach of merging microgrids has great potential for restoring distribution networks. To make this possible, however, one needs to consider the interdependence of the electrical and the communication infrastructure.

C. Computation Times

MILP problems are known to be NP-hard, since they can, for example, model the knapsack problem. Computation times can thus be challenging, especially when large grid and numerous DGs greatly increase the number of binary variables and equations. In an online application for reactive grid restoration

acceptable computation times would depend on the speed of "slow" communication system to gather the input information and distribute the optimization results. They would also have to be set into perspective of the startup times of the DGs. We conclude that times in the range of a few minutes should be acceptable in most cases.

On a laptop with an Intel I5-8265U processor and 16 GB RAM the 5-node test grid solves in less then a second. The IEEE 123-node test feeder takes more than one hour to obtain a proven gap of 1 %. However, a solution with a proven optimality gap of 9 % and 100 % load restoration in 9 timesteps is already found after 1:54 min.

This shows that the computations times, despite being significant, may be well-suited to solve realistic restoration tasks. If not all lines and loads are individually switchable – which will be the case for many grids in the near future – the number of variables is greatly reduced and faster computation times can be achieved.

V. Conclusion

In this paper we presented an approach for finding optimal restoration sequences for a smart distribution grid with black-start capable DGs and switchable lines and loads. The merging of multiple microgrids was made conditional on the availablility of an active communication link between the DGs to coordinate their joint operation. To this end, we explicitly took the topologies of the electric and the communication grid into account and formulated the problem as a MILP maximizing the restored load. The case studies supported the claim that cooperative DG operation enables supplying larger and potentially more critical loads.

Further work might consider incomplete situational awareness during the restoration process, especially schemes where the individual microgrids act on their own to quickly recover as much load as possible, but still are able to actively coordinate and merge with neighboring microgrids when these are discovered.

Acknowledgment

This work has been funded by the LOEWE initiative (Hesse, Germany) within the emergenCITY centre.

References

[1] X. Fang, S. Misra, G. Xue, and D. Yang, "Smart grid—the new and improved power grid: A survey," *IEEE communications surveys & tutorials*, vol. 14, no. 4, pp. 944–980, 2011.

[2] A. Hahn and M. Govindarasu, "Cyber attack exposure evaluation framework for the smart grid," *IEEE Transactions on Smart Grid*, vol. 2, no. 4, pp. 835–843, 2011.

[3] E. I. Sharing and A. C. (E-ISAC), "Analysis of the cyber attack on the ukrainian power grid," 2016.

[4] P. Hoeppe, "Trends in weather related disasters – consequences for insurers and society," *Weather and Climate Extremes*, vol. 11, pp. 70–79, 2016.

[5] International Electrotechnical Commision, "Microgrids for disaster preparedness and recovery: With electricity continuity plans and systems," Genf, 2014.

[6] H. Aki, "Demand-side resiliency and electricity continuity: Experiences and lessons learned in japan," *Proceedings of the IEEE*, vol. 105, no. 7, pp. 1443–1455, 2017.

[7] C. Chen, J. Wang, F. Qiu, and D. Zhao, "Resilient distribution system by microgrids formation after natural disasters," *IEEE Transactions on Smart Grid*, vol. 7, no. 2, pp. 958–966, 2016.

[8] B. Chen, C. Chen, J. Wang, and K. L. Butler-Purry, "Sequential service restoration for unbalanced distribution systems and microgrids," *IEEE Transactions on Power Systems*, vol. 33, no. 2, pp. 1507–1520, 2018.

[9] A. Arif, Z. Wang, C. Chen, and J. Wang, "Repair and resource scheduling in unbalanced distribution systems using neighborhood search," *IEEE Transactions on Smart Grid*, vol. 11, no. 1, pp. 673–685, Jan 2020.

[10] S. Lei, C. Chen, Y. Li, and Y. Hou, "Resilient disaster recovery logistics of distribution systems: Co-optimize service restoration with repair crew and mobile power source dispatch," *IEEE Transactions on Smart Grid*, vol. 10, no. 6, pp. 6187–6202, 2019.

[11] UO Team, "Ucte oh entsoe operations handbook," 2004. [Online]. Available: https://www.entsoe.eu/publications/system-operations-reports/continental-europe-operation-handbook

[12] J. W. Simpson-Porco, F. Dörfler, and F. Bullo, "Synchronization and power sharing for droop-controlled inverters in islanded microgrids," *Automatica*, vol. 49, no. 9, pp. 2603–2611, 2013.

[13] J. Börner and F. Steinke, "Distributed secondary frequency control via price consensus," in *2018 IEEE PES Innovative Smart Grid Technologies Conference Europe (ISGT-Europe)*, Oct 2018, pp. 1–6.

[14] F. Álvarez, L. Almon, H. Radtki, and M. Hollick, "Bluemergency: Mediating post-disaster communication systems using the internet of things and bluetooth mesh," *ArXiv*, vol. abs/1909.08094, 2019.

[15] ITU-T/ITU-R/ISO/IEC, "Frequency arrangements for public protection and disaster relief radiocommunication systems in accordance with resolution 646," 2018. [Online]. Available: https://www.itu.int/dms_pubrec/itu-r/rec/m/R-REC-M.2015-2-201801-I!!PDF-E.pdf

[16] X. Chen, W. Wu, and B. Zhang, "Robust restoration method for active distribution networks," *IEEE Transactions on Power Systems*, vol. 31, no. 5, pp. 4005–4015, 2016.

[17] B. Chen, Z. Ye, C. Chen, and J. Wang, "Toward a milp modeling framework for distribution system restoration," *IEEE Transactions on Power Systems*, vol. 34, no. 3, pp. 1749–1760, 2019.

[18] S. Lei, C. Chen, Y. Song, and Y. Hou, "Radiality constraints for resilient reconfiguration of distribution systems: Formulation and application to microgrid formation," 2019. [Online]. Available: http://arxiv.org/pdf/1907.04951v1

[19] G. Byeon, P. Van Hentenryck, R. Bent, and H. Nagarajan, "Communication-constrained expansion planning for resilient distribution systems," *arXiv preprint arXiv:1801.03520*, 2018.

[20] Z. Wang, B. Chen, J. Wang, and C. Chen, "Networked microgrids for self-healing power systems," *IEEE Transactions on Smart Grid*, vol. 7, no. 1, pp. 310–319, 2016.

[21] S. Lei, C. Chen, Y. Song, and Y. Hou, "Radiality constraints for resilient reconfiguration of distribution systems: Formulation and application to microgrid formation," 2019. [Online]. Available: http://arxiv.org/pdf/1907.04951v1

[22] M. Lavorato, J. F. Franco, M. J. Rider, and R. Romero, "Imposing radiality constraints in distribution system optimization problems," *IEEE Transactions on Power Systems*, vol. 27, no. 1, pp. 172–180, 2012.

[23] T. Ding, K. Sun, C. Huang, Z. Bie, and F. Li, "Mixed-integer linear programming-based splitting strategies for power system islanding operation considering network connectivity," *IEEE Systems Journal*, vol. 12, no. 1, pp. 350–359, 2018.

[24] A. Arif, Z. Wang, C. Chen, and B. Chen, "A stochastic multi-commodity logistic model for disaster preparation in distribution systems," *IEEE Transactions on Smart Grid*, vol. 11, no. 1, pp. 565–576, Jan 2020.

[25] B. Stott, "Review of load-flow calculation methods," *Proceedings of the IEEE*, vol. 62, no. 7, pp. 916–929, 1974.

[26] IEEE PES Power System Analysis, Computing, and Economics Committee, "Ieee 123 node test feeder," 2014. [Online]. Available: http://site.ieee.org/pes-testfeeders/files/2017/08/feeder123.zip

[27] G. D. Corporation, "General Algebraic Modeling System (GAMS) Release 25.1.3," Fairfax, VA, USA, 2018. [Online]. Available: http://www.gams.com/